

A Performance Analysis For An Air-Pollution Monitoring Using A Pulsed Dye Laser

Hiroya SANO*, Ryuji KOGA*, Yoshihiro TANADA*
and Megumi KOSAKA*

(Received February 7, 1979)

Synopsis

The maximally attainable accuracy of an air-pollution monitoring system is investigated. The system is composed of a tunable pulsed dye laser as the light source, photodiodes as the opto-electric converter and a low noise electronic signal processor specifically designed by the authors. The extreme value of the accuracy is given in terms of the standard deviation of the attenuation. The value is $3.4 \times 10^{-4} [\text{Nep} \sqrt{\text{pulse number}}]$ for an averaged value for multiple laser shots.

Also the wavelength reproduceability of a dye laser was examined, which resulted in that a computer should take a part in the wavelength control in order that this method should be feasible.

1. Introduction

Raman scattering methods¹⁾ had revealed to fail in gaseous air-pollution monitoring due to its inherently small Raman cross sections of the pertaining gas molecules. The resonance absorption whose cross section is several orders larger than that of Raman, realizes a system that may achieve a real-time and sensitive air-pollution monitoring²⁾.

Inevitable pulsed features of available high powered tunable lasers give rise to the idea of laser radar configuration with long light pathlength, which can detect a few parts per billion of densi-

* Department of electronics

ties for chromatic gaseous air pollutants.

Application of the resonance absorption to a system which measures the absorption over a short pathlength, l [m], for instance, has been explained to be, however, impossible due to the noise arising in the pertaining electric and electronic apparatuses³⁾.

The authors have been occupied in the development of the electronic apparatuses which deal with electronic pulse signal in high signal to noise ratio^{4,5)}. Their experience led to an attempt to examine the feasibility of the short-pathlength system for a point gas analyzer which is compact and gives local gas densities.

This report deals with the minimal noise that may arise in the light attenuation measurement for practical values of parameters. Also experiments have been made by a specifically built apparatus including a pulsed dye laser. Difference between theoretical results and that by experiments is attributed to the persisting electromagnetic impulsive noise. Earlier results of this subject have been reported in Japanese⁶⁾, but more convincing results are added along with the discussions on the wavelength reproducibility which implies the span-accuracy deterioration in the resulting density values based on the experimental data.

2.1 Principles and apparatuses used in experiments

Nitric Oxide(NO), sulfur dioxide(SO₂) and ammonia(NH₃) have distinct absorption lines commonly in the 220-230 nm wavelength region, whereas other atmospheric constituents have rather continuous and smooth spectral profiles there.

Let a monochromatic pulsed laser light of energy p_I and wavelength λ be transmitted in polluted atmosphere over a path length L , to be attenuated to energy p_T . Lambert-Beer's law implies

$$\tau(\lambda) \equiv \ln(p_I/p_T) = \sum_{i \in I} \alpha c_i L s_i(\lambda), \quad (1)$$

where τ is hereafter nominated as "attenuation" and c_i , s_i are the density in parts per million and the absorption cross section of the i -th species, respectively. The coefficient α appears by replacing the molecular number density N_i with the density c_i .

Employment of adjoint spectra⁷⁾ leads to

$$c_j = \frac{1}{\alpha L} \int_{\Lambda} s_j^*(\lambda) \cdot \bar{\tau}(\lambda) \cdot d\mu(\lambda), \quad (2)$$

which stands for a numerical filter for the measured absorption spectrum $\bar{\tau}$. The notion of the adjoint spectra was introduced by the authors extending the well-known method of least squares.

A measured absorption spectrum is inevitably associated with random noise n , as

$$\bar{\tau} = \tau + n. \quad (3)$$

If the noise has no correlation with the wavelength nor with time instance, the variance of the obtained density \tilde{c}_j becomes

$$\text{Var}(\tilde{c}_j) = \frac{\text{Var}(n)}{(\alpha L)^2} \int_{\Lambda} \{s_j^*(\lambda)\}^2 d\mu(\lambda). \quad (4)$$

This expression suggests that the variance depends on the specific adjoint spectrum employed. The adjoint spectrum is not unique. The variance of n is the value characteristic to a specific instrument and is governed by a principle and the functioning elements employed therein. A purpose of this paper is to give the $\text{Var}(n)$ value.

2.2 Description of the examined apparatus

Optical schematic diagram is shown in **Fig.1**.

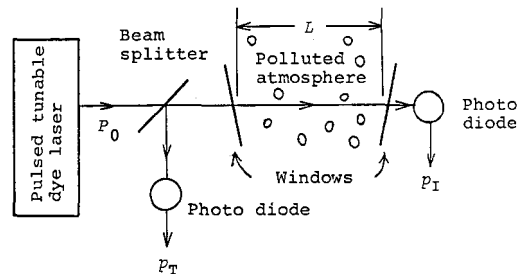


Fig.1 Schema of the short path absorption method for the point air-pollution monitoring.

The beam from a pulsed dye laser is splitted into two. One is monitored by a photo-diode to yield a charge Q_I which stands for the energy of the incident light pulse. The other goes through polluted atmosphere of path L and is led to another photo-diode to give charge Q_T , viz.,

$$\exp(-\bar{\tau}) = Q_T/Q_I = \exp(-\xi) \cdot \exp(-\tau), \quad (5)$$

where the factor $\exp(-\xi)$ stands for an unbalance between the composite optical and electrical efficiency of the two signal path.

It is, however, improper to normalize Q_T by Q_I directly when $\bar{\tau}$ is small, which requires a large number of bits in the analog to digital conversion prior to the division carried out by a digital computer and also requires the electronic circuits for impossibly large dynamic range.

In order to circumvent this difficulty, a particular circuit configuration was devised by the authors⁵⁾. The system named as the instantaneous difference compensation (IDC) system, deals with the difference signal, $Q_I - Q_T$ and the normalizing signal, Q_I , instead of Q_T and Q_I . The $\bar{\tau}$ value is given as

$$\bar{\tau} = \ln \frac{Q_I}{Q_T} = \frac{Q_I - Q_T}{Q_I}. \quad (6)$$

When $\bar{\tau}$ is much smaller than unity, this approximation becomes correct and the range that $Q_I - Q_T$ spans small, or rather small dynamic range is required for the amplifier for the difference signal. A blockdiagram is shown as **Fig.2**.

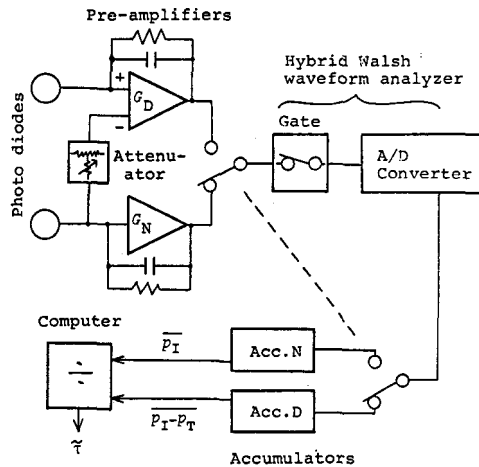


Fig.2 A Blockdiagram of the electronic signal processor based on the IDC system.

The gate functions as a time window of one microsecond duration, which suppresses the stationary shot noise induced by the background light and the dark current of the photodiode.

A part of the electronic circuits is mutually shared by the differential and the normal signals in order to reduce the number of elements and to retain some consistency between the two signals. Actually the gating function was performed by a hybrid Walsh waveform analyzer which had been developed by a part of the authors⁴⁾.

3. Schemes for noise suppression and its effects

3.1 Mechanical vibration of the optical system

Angle perturbation of optical elements results in the fluctuation of ξ in Eq. (5). When an optical surface is in near right angle with the incident light, this effect is small. The vibration of the beam-splitting surface is, therefore, the leading element for this effect. If the incident light beam is linearly polarized, the reflectance R is determined by the incidence angle ϑ , the polarization angle ϕ and the index of refraction n of the semi-transparent layer. For a particular values of the parameters, an equation

$$\frac{d}{d\vartheta} R(\vartheta, \phi, n) = 0 \tag{7}$$

holds, which means that a proper choice of the parameters gives rise to an immunity against mechanical vibration. The solutions of Eq. (7) are given by **Fig. 3**, where the values of R are associated as well.

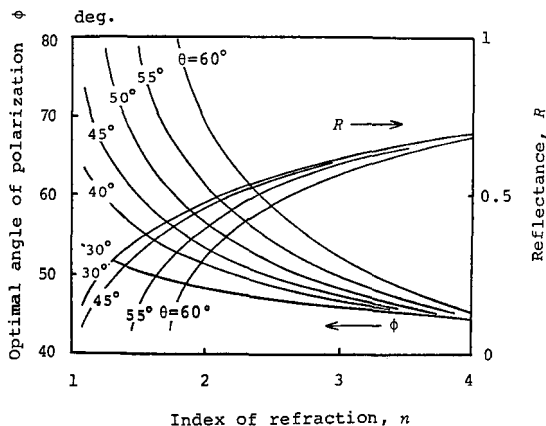


Fig. 3 Optimal angle ϕ between the incident and the polarization planes w.r.t. the index of refraction n , for some incidence angles ϑ . Resulting reflectance, R , are associated.

Fig. 4 Experimental result for the effect of the polarization angle of the incident light.

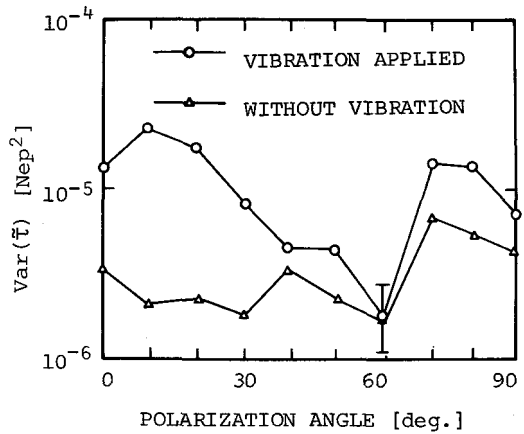


Figure 4 is the results of an experiment to exemplify this effect. The incident light is linearly polarized by a polarized filter whose extinction ratio is below 10^{-3} . A beamsplitting cube was used, whose transmission ratios were more than 45% for both transparent and reflected beam. The cube was put on a cloth cushion which offers an intentional, unstable suspension, and the optical bench was vibrated by an electric motor. Distinct rejection for vibration-induced fluctuation is seen at $\varphi=60^\circ$. The angle setting was very critical to find the optimal angle.

3.2 Laser power fluctuation and the IDC system

The laser power fluctuates from each pulse to another and with long time duration. As the tunable light source, a dye laser which is pumped by a pulsed nitrogen laser is used. Rating energy is 0.7 [mJ] per pulse at 10 [pps] when dye, 7D4MC, is used as active medium. Figure 5 shows energies of each pulse of the laser output and Fig. 6, long time transition.

Fig. 5 A record of laser output energy of every pulse.

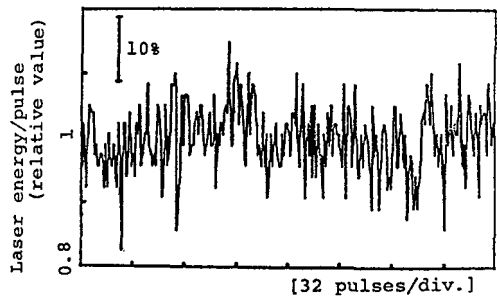
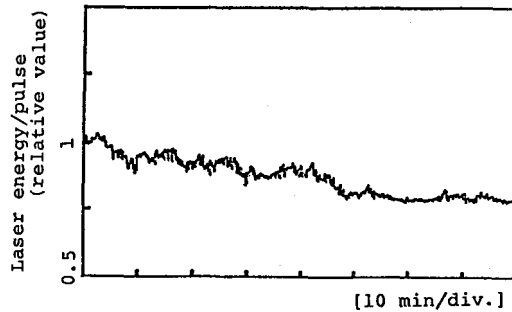


Fig. 6 A long time record of the laser output.



The laser energies are transformed to electric pulse heights by a photo-diode, and are fed to a digital waveform recorder. The fluctuation is decomposed into two constituents: the gaussian which has no correlation between each pulses, and another, which has a $1/f$ feature including drift term. This is clearly seen in **Fig. 7** which shows the resulting $\text{Var}(\bar{\tau})$ versus m , the number of accumulation for both the difference and the normalizing signal prior to the normalization. The vertical axis is scaled in $m \cdot \text{Var}(\bar{\tau})$. When m is small, the curve is parallel to the abscissa, which depicts the ergodic feature of the noise. The curve, however, rises up as m increases, which is attributed to the non-ergodic component in the noise.

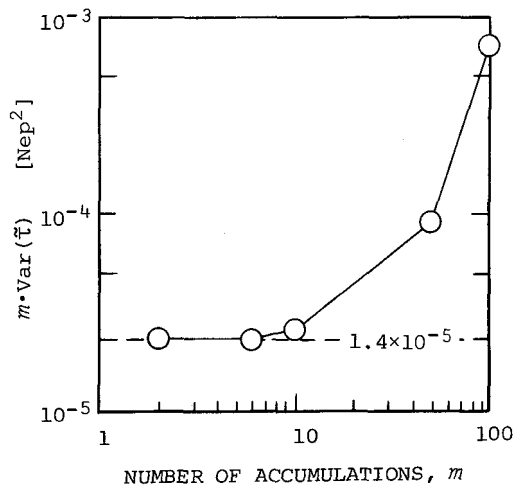


Fig. 7 Dependence of $m \cdot \text{Var}(\bar{\tau})$ on the number of accumulation, m .

Residual noise of the IDC system due to the laser power fluctuation becomes

$$\text{Var}(x_{\text{IDC}}) = 2(1-\xi)^2 \text{Var}(x_p), \tag{8}$$

where x_p stands for the relative fluctuation of the laser power around its average value. The IDC residue, Eq. (8), is attributed to that the

difference and the normalizing signals are generated for the alternating laser shots respectively in order to reduce the number of electronic components. Full performance of the IDC system is, therefore, attained for ξ of unity.

3.3 Noise in opto-electronic conversion and in the signal processing

A photo-diode generates a stationary noise, which is of the shot noise induced by the DC current, and of the thermal noise. Taking the internal noise of the preamplifier into account by a notion of the noise figure, a power spectral density p of the noise current that flows through the load resistor becomes

$$p = 2q(I_B + I_0) + 4FkT/R_L, \tag{9}$$

where the variables stand for

- q : the charge of an electron,
- I_B : background current,
- I_0 : dark current,
- R : load resistance,
- T : absolute temperature,
- k : Boltzmann's constant,
- F : a noise figure of the pre-amplifier.

Utilization of a time window with short time duration along with a pulsed laser makes it possible to reduce that stationary noise. Let x_e be the ratio of the fluctuation of the output voltage of the system illustrated in **Fig.8**, to that of the averaged value.

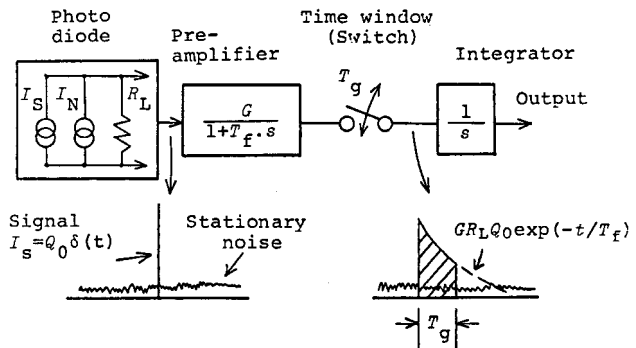


Fig.8 Suppression of stationary noise by a time window and an integrator.

The variance of x_p is calculated from a theory about the integral of random signal over a definite time interval⁸⁾ as

$$\text{Var}(x_p) = \frac{pT_f}{(\eta N_p q)} \frac{x + e^{-x} - 1}{(1 - e^{-x})}, \quad (10)$$

where x stands for the ratio of T_g to T_f .

The data processing by a computer requires the analog to digital conversion, which implies the quantization noise as

$$\text{Var}(x_{AD}) = \frac{1}{12} (\tau_{\max})^2 \cdot 2^{-2M}, \quad (11)$$

where τ_{\max} : the full scale of τ value of the AD converter,

M : number of bits of the digital output signal.

The corpuscular feature of light results in the shot noise in the signal charge, as

$$\text{Var}(x_q) = \frac{1 - \eta}{\eta N_p}, \quad (12)$$

where

x_q : the relative fluctuation in the signal charge that is induced by the photo-conductive phenomenon for an incident light pulse,

η : the quantum efficiency of the photodiode,

N_p : the number of photons of the incident light pulse.

3.4 Numerical and experimental results

Parameters of the apparatus built for test are listed in **Table 1**, and values of $\text{Var}(\bar{\tau})$ calculated by these parameters, in **Table 2**. By the experiment, it was found to be difficult to control the unbalance $|1 - \xi|$ within 10^{-2} , due to technical difficulties in electronic circuits. If the fluctuation in $\bar{\tau}$ is Gaussian, the variance of $\bar{\tau}$ reduces to $1/m$ by averaging m laser shots. Taking this IDC residue into account, the theoretical evaluation gives the variance of $\bar{\tau}$ as 3.4×10^{-4} [$\text{Nep}^2 \cdot m$], whereas it should be 1.15×10^{-7} [$\text{Nep}^2 \cdot m$] for a hypothetical function to reduce the unbalance of IDC.

The experiment resulted in the variance of about 1.8×10^{-5} [$\text{Nep}^2 \cdot m$], whereas the value was 1.0×10^{-6} [$\text{Nep}^2 \cdot m$] for a simulation in that the photo-diodes were replaced by an electric pulse generator and the laser system was stopped because it radiates intensive electro-magnetic impulse noise around it despite its careful shields. The difference between the two values are considered to be of the IDC residue

and the electromagnetic noise.

Table 1 Parameters for the calculation of the fluctuation in \bar{f} .

SNR in laser loutput	$\sigma^2(x_p)$	2.21×10^{-3}	
Photon numbers of incident light	N_p	1.5×10^9	(a)
Photo diodes			
Quantum efficiency	η	0.3	
Dark current	I_0	1 μ A	
Background light current	I_B	25 μ A	
Load resistance	R_L	$2 \times 10^3 \Omega$	
Pre-amplifier			
Noise figure	F	10	(b)
Corner frequency	$1/T_f$	1 MHz	
Aperture time of the time window	T_g	1 μ s	
Analog to digital converter			
Full scale	τ_{max}	10^{-2}	
Number of bits	M	8	
Inherent unbalance of the IDC	$\Delta \xi$	10^{-2}	(c)
Ambient temperature	T	295 K	

(a) Limited by the range of linearity.

(b) A presumable practical value.

(c) Empirical value through the experiment.

Table 2 Fluctuation in \bar{f} calculated from the Table 1.

Terms	Eqs.	Var(\bar{f}) [$\times \frac{1}{4} \text{Nep}^2$]
IDC residue	(8)	4.42×10^{-7}
Shot noise		
by signal	(12)	1.56×10^{-9}
by background light and dark current	(9), (10)	1.42×10^{-9}
Thermal and amplifier noise	(9), (10)	1.44×10^{-8}
Quantization noise in AD conversion	(11)	1.27×10^{-10}
Total		4.6×10^{-7}

4. Wavelength reproducibility of the dye laser

A wavelength deviation $\delta\lambda_k$ from a prescribed value $\bar{\lambda}_k$ causes an error in the final result of c_i after the numerical filter, viz.,

$$\delta c_i = \sum_{i \in I} s_{ik}^* \delta \tau_i(\lambda_k), \quad (13)$$

where the integration and the adjoint spectrum are replaced by the summation and s_{ik}^* , respectively. The suffix k stands for the pertaining wavelength λ_k .

Taking only a species of gas absorption spectrum into consideration, the $\delta s_i(\lambda_k)$ is denoted as

$$\delta s_i(\lambda_k) = s_i'(\bar{\lambda}_k) \delta \lambda + \frac{1}{2} s_i''(\bar{\lambda}_k) \cdot (\delta \lambda_k)^2 + \dots \quad (14)$$

In order for δs_i be zero for a $\delta \lambda_k$, the nominal wavelengths $\bar{\lambda}_k$, $k \in K$ should be chosen so that an equation

$$s_i'(\lambda_k) = 0 \quad (15)$$

holds, which reduce the effect from the inherent error in wavelength setting. After this has been performed, the second term of Eq. (14) becomes dominant.

The dye laser employed in this experiment is equipped with a grating as the tuning facility, which is driven by a step-motor according to digital signals from a computer. However a manual establishment of the initial wavelength on the system startup is necessitated.

The spectral profile of the $\gamma(0,0)$ band of nitric oxide is composed of discrete and separated lines each of which corresponds to a specific electronic transition and rotational-vibrational sublevel⁹⁾. Repeated measurements of the spectrum for a line results in the wavelength accuracy within 0.04 cm^{-1} of standard deviation with the step-motor control. This line is of Q(15) branch of the electronic $A^2\Sigma^+ - X^2\Pi_{1/2}$ transition. The reproducibility of the manual wavelength setting on the system startup is within a few kayser which is enough small to identify each absorption line of nitric oxide. By comparing the line profile of the measured with that given by Tajime *et al.*⁹⁾, the line profile is revealed to be governed by the laser power spectral profile rather than that of nitric oxide.

The absorption spectra of ammonia and sulfur dioxide under the atmospheric pressure are taken also, both revealed to be of continuous spectra. This is compatible with the line profile in infrared region taken by a ultra-high resolution diode spectrometer¹⁰⁾.

Typical values of $\beta = \frac{1}{2} s''_i(\lambda_k)$ for the three gases are listed in **Table 3**, which implies that the $\delta \tilde{\nu}_i$ value determined by Eq.(13) takes some dozens percents of the rated $\tilde{\nu}$ value for a wavelength error introduced by manual setting. The error from the step-motor control is, however, much less than this. An algorithmic wavelength control executed by a computer is, therefore, necessary and will enables the system to obtain a value of $\tilde{\nu}(\lambda_k)$ that is free from an error induced by the wavelength missettings. The volume of the program is considered to be moderate for the installation to a microcomputer, though are they not made practically.

Table 3 Values of β for characteristic peaks of NO, SO₂ and NH₃ spectra.

Gas species	Wavelength [nm]	β [(pm) ²]
NO	$\gamma(0,0)$ band	1.26×10^{-1}
NH ₃	224.47	8.75×10^{-3}
SO ₂	225.75	1.98×10^{-3}

5. Concluding remarks

The attainable accuracy of the short pass absorption measurement is 3.4×10^{-4} [Nep · $\sqrt{\text{pulse number}}$] of the standard deviation, which is still dominated by an error in the specific electric-circuit configuration, IDC system, which is developed by the authors. The value corresponds to 0.63 [ppm · m · $\sqrt{\text{pulse number}}$] for the density measurement for nitrogen dioxide at wavelength of 462.8 [nm].

The wavelength reproduceability of the dye-laser employed is tolerable on the assumption that a computer pertains to the wavelength control.

The principal direction to further reduce the fluctuation in an obtained density values is to use a photo-diode which may respond linearly to a light pulse of higher energy. The difficulty in the wavelength reproduceability can be overcome by an employment of a reference cell which contains pure nitric oxide in reduced pressure.

References

- 1) H. Inaba: *Laser Monitoring of the Atmosphere* (E.D. Hinkley, Ed.), (Springer, 1976), p.153.
- 2) R. L. Byer and M. Garbuny: *Appl. Opt.*, **12**(1973).
- 3) T. Tsuji, H. Kimura, Y. Higuchi and K. Goto: *Jap. J. Appl. Phys.*, **15**(1976) 1743.
- 4) Y. Tanada, and H. Sano: *Trans. IECE*, **J59-A**(1976) 101(in Japanese).
- 5) H. Sano, Y. Tanada, R. Koga and T. Ono: *J. Illum. Eng. Inst. Jap.*, **61**(1977) 35 (in Japanese).
- 6) H. Sano, R. Koga, and Y. Tanada: to be published in *Trans. Soc. Inst. Contr. Eng.* (in Japanese).
- 7) R. Koga, Y. Tanada, H. Sano: *J. Spectroscop. Soc. Jap.*, **27**(1978) 297(in Japanese).
- 8) W. B. Davenport, Jr., and W. L. Root: *An Introduction to The Theory of Random Signal And Noise*, (McGraw-Hill, 1958).
- 9) T. Tajime, T. Saheki, and K. Ito: *Appl. Opt.*, **17**(1978) 1290.
- 10) G. A. Antcliffe and J. S. Wrobel: *Appl. Opt.*, **11**(1971) 1543.